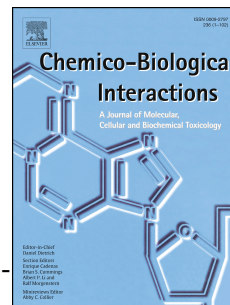


# Accepted Manuscript

Inhibition of human carboxylesterases by magnolol: Kinetic analyses and mechanism

Yun-Qing Song, Zi-Miao Weng, Tong-Yi Dou, Moshe Finel, Ya-Qiao Wang, Le-Le Ding, Qiang Jin, Dan-Dan Wang, Sheng-Quan Fang, Yun-Feng Cao, Jie Hou, Guang-Bo Ge



PII: S0009-2797(19)30481-8

DOI: <https://doi.org/10.1016/j.cbi.2019.06.003>

Reference: CBI 8690

To appear in: *Chemico-Biological Interactions*

Received Date: 19 March 2019

Revised Date: 22 May 2019

Accepted Date: 3 June 2019

Please cite this article as: Y.-Q. Song, Z.-M. Weng, T.-Y. Dou, M. Finel, Y.-Q. Wang, L.-L. Ding, Q. Jin, D.-D. Wang, S.-Q. Fang, Y.-F. Cao, J. Hou, G.-B. Ge, Inhibition of human carboxylesterases by magnolol: Kinetic analyses and mechanism, *Chemico-Biological Interactions* (2019), doi: <https://doi.org/10.1016/j.cbi.2019.06.003>.

This is a PDF file of an unedited manuscript that has been accepted for publication. As a service to our customers we are providing this early version of the manuscript. The manuscript will undergo copyediting, typesetting, and review of the resulting proof before it is published in its final form. Please note that during the production process errors may be discovered which could affect the content, and all legal disclaimers that apply to the journal pertain.

1 **Research paper**

2

3 **Inhibition of human carboxylesterases by magnolol: kinetic analyses and**  
4 **mechanism**

5

6 Yun-Qing Song <sup>1</sup>, Zi-Miao Weng <sup>2</sup>, Tong-Yi Dou <sup>3</sup>, Moshe Finel <sup>4</sup>, Ya-Qiao Wang <sup>1</sup>, Le-Le Ding <sup>1</sup>, Qiang  
7 Jin <sup>1</sup>, Dan-Dan Wang <sup>1</sup>, Sheng-Quan Fang <sup>1</sup>, Yun-Feng Cao <sup>5</sup>, Jie Hou <sup>2,\*</sup>, Guang-Bo Ge <sup>1,\*</sup>

8

9 <sup>1</sup> Translational Medicine Center, Yueyang Hospital of Integrated Traditional Chinese and Western  
10 Medicine & Institute of Interdisciplinary Integrative Medicine Research, Shanghai University of  
11 Traditional Chinese Medicine, Shanghai, 200473, China.

12 <sup>2</sup> Department of Biotechnology, College of Basic Medical Sciences, Dalian Medical University, Dalian  
13 116044, China.

14 <sup>3</sup> School of Life Science and Medicine, Dalian University of Technology, Panjin 124221, China.

15 <sup>4</sup> Division of Pharmaceutical Chemistry and Technology, Faculty of Pharmacy, University of Helsinki,  
16 00014, Finland.

17 <sup>5</sup> Dalian Runsheng Kangtai Medical Laboratory Co.Ltd, Dalian, China

18

19

20 \*Corresponding author

21 E-mail address: geguangbo@dicp.ac.cn (G.-B. Ge); houjie@nankai.edu.cn (J. Hou).

22 **Abstract**

23 Magnolol, the most abundant bioactive constituent of the Chinese herb *Magnolia*  
24 *officinalis*, has been found with multiple biological activities, including anti-oxidative,  
25 anti-inflammatory and enzyme-regulatory activities. In this study, the inhibitory effects and  
26 inhibition mechanism of magnolol on human carboxylesterases (hCEs), the key enzymes  
27 responsible for the hydrolytic metabolism of a variety of endogenous esters as well as  
28 ester-bearing drugs, have been well-investigated. The results demonstrate that magnolol  
29 strongly inhibits hCE1-mediated hydrolysis of various substrates, whereas the inhibition of  
30 hCE2 by magnolol is substrate-dependent, ranging from strong to moderate. Inhibition of  
31 intracellular hCE1 and hCE2 by magnolol was also investigated in living HepG2 cells, and  
32 the results showed that magnolol could strongly inhibit intracellular hCE1, while the  
33 inhibition of intracellular hCE2 was weak. Inhibition kinetic analyses and docking  
34 simulations revealed that magnolol inhibited both hCE1 and hCE2 in a mixed manner, which  
35 could be partially attributed to its binding at two distinct ligand-binding sites in each  
36 carboxylesterase, including the catalytic cavity and the regulatory domain. In addition, the  
37 potential risk of the metabolic interactions of magnolol *via* hCE1 inhibition was predicted on  
38 the basis of a series of available pharmacokinetic data and the inhibition constants. All these  
39 findings are very helpful in deciphering the metabolic interactions between magnolol and  
40 hCEs, and also very useful for avoiding deleterious interactions *via* inhibition of hCEs.

41

42 **Keywords:** Magnolol; Human carboxylesterases (hCEs); Inhibition potential; Herb-drug  
43 interactions (HDIs)

## 44 1. Introduction

45 *Magnolia officinalis* (also named Houpo in Chinese), an edible herbal medicine, has been  
46 frequently used for the treatment of gastrointestinal disorders, anxiety, asthma and cough, in  
47 Asian countries. In China, a variety of prescriptions containing Houpo are used in modern  
48 clinical practice for their sedative, anti-inflammatory, antibiotic, and antispastic effects [1]. In  
49 Japan, some herbal medicines containing *Magnolia* bark, such as Hange-Koboku-To and  
50 Saiboku-To, are also used in modern clinical practice [2, 3]. Furthermore, the concentrated  
51 *Magnolia* bark extracts (MBEs, containing more than 92% magnolol) have been approved as  
52 an active ingredient for preparing dietary supplements and cosmetics [4, 5]. Although MBEs  
53 and its major constitute magnolol (5,5'-diallyl-2,2'-biphenyldiol; **Fig 1**) displayed good  
54 safety profile, recent investigations have demonstrated that magnolol could affect the  
55 pharmacokinetic behavior of some therapeutic drugs *via* inhibition of a panel of human drug  
56 metabolizing enzymes, including cytochrome P450 enzymes (CYPs) and  
57 UDP-glucuronosyltransferases (UGTs) [6, 7]. Considering that MBEs are commonly added to  
58 foods (such as mints and chewing gums), as well as cosmetic products [5, 8], human could be  
59 easily exposed to magnolol at high doses in daily life. Therefore, it is important to carefully  
60 investigate the interactions of magnolol with drug metabolizing enzymes before the  
61 combined use of MBEs and clinical drugs.

62 As mentioned above, regulatory effects of magnolol on CYPs and UGTs have been  
63 reported already [6, 7], but the interactions of magnolol with other key drug metabolizing  
64 enzymes in human, such as the esterases, have not been well-examined. Mammalian esterases  
65 are pivotal serine hydrolases that are expressed in metabolic organs and catalyze the cleavage

66 of important ester, amide or thioester bonds within a wide variety of compounds [9, 10].  
67 Esterases contribute to the metabolism of about 10% of the total clinical drugs that contain  
68 ester or amide bonds [11]. In mammals, carboxylesterases (CEs) are the most abundant  
69 esterases in metabolic organs (such as liver, intestine and kidney), and play key roles in the  
70 hydrolytic metabolism of a variety of endogenous esters and xenobiotics bearing ester bonds.  
71 In the human body, human carboxylesterase 1 (hCE1) and carboxylesterase 2 (hCE2) have  
72 been identified as the predominant CE isoforms and they are involved in detoxification of  
73 ester toxins and the hydrolysis of many ester drugs or prodrugs, including clopidogrel,  
74 oseltamivir, irinotecan and capecitabine [12, 13]. Inhibition of hCEs may slow down the  
75 hydrolysis of their substrate drugs *in vivo*, thereby modulating the outcomes of these drugs.  
76 For instance, the primary metabolite of clopidogrel (one of the most frequently prescribed  
77 antiplatelet drugs) is the inactive clopidogrel carboxylic acid that is generated by hepatic  
78 hCE1 [14]. Upon addition of hCE1 inhibitors, clopidogrel hydrolysis may be partially  
79 blocked, while the plasma levels of both clopidogrel and its active metabolite that is activated  
80 by several hepatic CYPs could rise to too high levels [15]. Another interesting and important  
81 example is CPT-11 (also named irinotecan), an anti-cancer prodrug that can be activated by  
82 hCE2 to the active metabolite SN-38. Accumulation of SN-38 in the gastrointestinal system  
83 can trigger severe delayed diarrhea that may even be life threatening. It is suggested that  
84 co-administration of irinotecan with potent hCE2 inhibitors may ameliorate its associated  
85 life-threatening diarrhea, and thereby improve the quality of the patient's life [16-19].

86 In addition to xenobiotic metabolism, human CEs, particularly hCE1, play crucial roles in  
87 endogenous metabolism. Recent investigations have demonstrated that hCE1 is a key enzyme

88 responsible for hydrolysis of endogenous esters (such as cholesteryl esters), thus playing  
89 central roles in energy metabolism-related processes, such as lipid metabolism and  
90 cholesterol homeostasis [20, 21]. Moreover, it was found that both hCE1 levels and its  
91 hydrolytic activities in the adipose tissues from type 2 diabetic and obese patients are  
92 elevated when compared with lean healthy subjects [22]. Upon addition of CE1 inhibitors,  
93 some beneficial effects to metabolic features were observed in type 2 diabetic mice [22].  
94 These findings highlight the importance of hCEs in both endogenous and xenobiotic  
95 metabolism and raise much interest in the discovery of more potent hCEs modulators with  
96 good safety profiles to regulate hCEs-associated endogenous metabolism, or improve  
97 treatment outcomes of hCEs substrate drugs.

98 In the present study, the metabolic interactions of magnolol with the human CE1 and CE2 were  
99 carefully investigated in human liver microsomes (HLM) and in living cells. For this purpose,  
100 two isoform-specific optical substrates, including D-luciferin methyl ester (DME, a hCE1  
101 substrate) and fluorescein diacetate (FD, a hCE2 substrate), were used for screening the  
102 inhibition of both hCE1 and hCE2 by magnolol. Subsequently, mechanistic insights into the  
103 interactions of magnolol with the hCEs were obtained by carefully characterizing the  
104 inhibition kinetics for both enzymes, using a panel of hCEs probe substrates (**Table S1**).  
105 Finally, docking simulations were also performed to gain deeper insights into the interactions  
106 of magnolol with both hCE1 and hCE2. These new findings added considerable information  
107 on the metabolic interactions between magnolol and hCEs, which was useful for the clinical  
108 pharmacists to reasonably use magnolol-containing products in order to avoid possible  
109 hCEs-mediated drug interactions.

## 110 2. Materials and methods

### 111 2.1 Materials

112 Magnolol was obtained from Dalian Meilun Biotech Co., Ltd (Dalian, China). The probe  
113 substrates for hCEs, including 3-O-*p*-ethylbenzoylflavone (3-EBF),  
114 N-(2-butyl-1,3-dioxo-2,3-dihydro-1*H*-phenalen-6-yl)-2-chloroacetamide (NCEN),  
115 2-(2-benzoyloxy-3-methoxyphenyl) benzothiazole (BMBT), DME and 3,5-Dimethyl  
116 BODIPY acid methyl ester (BME), were synthesized by the authors and the synthetic  
117 schemes have been depicted previously [23-27]. Fluorescein diacetate (FD), nevadensin and  
118 loperamide (LPA) were purchased from TCI (Shanghai, China). Clopidogrel and clopidogrel  
119 carboxylic acid (CCA) were obtained from Shanghai Boylechem Co., Ltd (Shanghai, China).  
120 Irinotecan and its hydrolytic metabolite 7-ethyl-10-hydroxycamptothecin (SN-38) were  
121 obtained from Tianjin Heowns Biochem LLC (Tianjin, China). The luciferin detection  
122 reagent (LDR) was purchased from Promega Biotech (Madison, USA). Magnolol and each  
123 substrate were dissolved in dimethyl sulfoxide (LC grade, Tedia, USA) to prepare stock  
124 solutions. Pooled human liver microsomes (HLMs, from 50 donors, lot no. X008067) were  
125 obtained from Bioreclamation IVT (Baltimore, MD, USA). Cell culture medium and fetal  
126 bovine serum were acquired from Hylcone (Logan, UK). HepG2 cell was purchased from the  
127 American Type Culture Collection (Teddington, Middlesex, UK). Phosphate buffered saline  
128 (0.1 M, pH 6.8 and pH 7.4), Millipore water and LC grade acetonitrile (Tedia, USA) were  
129 used for all experiments.

### 130 2.2 hCE1 inhibition assays

#### 131 2.2.1 Inhibition of hCE1-mediated DME hydrolysis by magnolol

132 A bioluminescent probe (DME) was used as an optical substrate for evaluating the  
133 inhibitory effects of magnolol on hCE1, while nevadensin (a specific hCE1 inhibitor) was  
134 used as a positive control [28]. Briefly, 91  $\mu\text{L}$  PBS (pH 6.8) was pre-mixed with 2  $\mu\text{L}$   
135 magnolol at different concentrations and 5  $\mu\text{L}$  HLM (1  $\mu\text{g}/\text{mL}$ ), and then pre-incubated at  
136 37  $^{\circ}\text{C}$  for 10 minutes. Subsequently, 2  $\mu\text{L}$  DME (3  $\mu\text{M}$ , final concentration) were added to the  
137 incubation system to start the reaction. After incubating at 37  $^{\circ}\text{C}$  in a shaking bath for 10  
138 minutes, all incubations were stopped by the addition of LDR (100  $\mu\text{L}$ ). A fluorescence  
139 microplate reader (SpectraMax® iD3, Molecular Devices, Austria) was used for  
140 luminescence measurements. The chemical structures of DME and its hydrolytic metabolite  
141 (D-luciferin), as well as the detection conditions are depicted in **Table S1**.

#### 142 *2.2.2 Inhibition of hCE1-mediated BME hydrolysis by magnolol*

143 BME, a newly developed fluorescent substrate for hCE1, was also used for evaluating the  
144 inhibitory effects of magnolol on hCE1. In brief, 194  $\mu\text{L}$  PBS (pH 7.4) was pre-mixed with 2  
145  $\mu\text{L}$  HLM (2  $\mu\text{g}/\text{mL}$ ) and 2  $\mu\text{L}$  magnolol at varying concentrations, and then pre-incubated at  
146 37  $^{\circ}\text{C}$  for 10 minutes in a shaking bath. BME (5  $\mu\text{M}$ ) was added to initiate the hydrolytic  
147 reaction. The hydrolytic metabolite of BME were real-time analyzed by a fluorescence  
148 microplate reader using excitation and emission wavelengths of 505 nm and 560 nm,  
149 respectively (Gain = 500). The kinetic parameters were set at 30 reads, with an interval of 60  
150 s and orbital shakes every 10 s before each read, at 37  $^{\circ}\text{C}$ . The chemical structures of BME  
151 and its hydrolytic metabolite, as well as the detection conditions are also depicted in **Table**  
152 **S1**.

#### 153 *2.2.3 Inhibition of hCE1-mediated BMBT hydrolysis by magnolol*



154 In brief, 194  $\mu\text{L}$  PBS (pH 7.4) was pre-mixed with 2  $\mu\text{L}$  HLM (2  $\mu\text{g}/\text{mL}$ ) and 2  $\mu\text{L}$   
155 magnolol at multiple concentrations, which was pre-incubated for 10 minutes at 37  $^{\circ}\text{C}$ . The  
156 reaction was initiated by the addition of BMBT (2  $\mu\text{M}$ , final concentration) and the mixture  
157 was further incubated for 20 min at 37  $^{\circ}\text{C}$  in a shaking bath. The reaction was terminated by  
158 the addition of ice-cold acetonitrile (200  $\mu\text{L}$ ), and the mixture was centrifuged at 20,000g for  
159 20 min at 4  $^{\circ}\text{C}$ . After that, aliquots of the supernatants were analyzed by LC-FD. The  
160 chemical structures of BMBT and its hydrolytic metabolite HMBT combined with the  
161 detection conditions of these two compounds were depicted previously [25].

#### 162 *2.2.4 Inhibition of hCE1-mediated clopidogrel hydrolysis by magnolol*

163 Considering that clopidogrel is a substrate drug for hCE1 and this drug has been frequently  
164 used in the clinic, the inhibitory effect of magnolol on hCE1-mediated clopidogrel hydrolysis  
165 was also investigated. Briefly, 194  $\mu\text{L}$  PBS (pH 7.4) was pre-mixed with 2  $\mu\text{L}$  HLM (50  
166  $\mu\text{g}/\text{mL}$ , final concentration) and 2  $\mu\text{L}$  magnolol at various concentrations, which was then  
167 pre-incubated for 10 minutes at 37  $^{\circ}\text{C}$ . The hydrolytic reaction was started by adding  
168 clopidogrel (6  $\mu\text{M}$ , final concentration) and the mixture was further incubated for 30 min at  
169 37  $^{\circ}\text{C}$  in a shaking bath. The reaction was terminated by adding 200  $\mu\text{L}$  of ice-cold  
170 acetonitrile containing 5-hydroxyflavone as the internal standard (IS, 0.5  $\mu\text{M}$ ). After  
171 centrifuged at 20,000  $\times g$  for 20 min at 4  $^{\circ}\text{C}$ , and the supernatant was diluted 10 times with  
172 acetonitrile for further analysis by LC-MS/MS. LC-MS/MS parameter for quantification of  
173 clopidogrel carboxylic acid as shown in **Table S2**. The detection conditions of clopidogrel  
174 and its hydrolytic metabolite CCA were depicted previously [28].

#### 175 *2.3 hCE2 inhibition assays*

176 *2.3.1 Inhibition of hCE2-mediated FD, 3-EBF and NCEN hydrolysis by magnolol*

177 Considering that hCE2 has multiple ligand-binding sites, different probe substrates,  
178 including FD, 3-EBF and NCEN, were used for studying the substrate-dependent inhibition  
179 of hCE2 by magnolol [29, 23, 24]. LPA was used as a positive hCE2 inhibitor in this study  
180 [30]. The chemical structures of FD, 3-EBF and NCEN and their site of hydrolysis by hCE2,  
181 as well as the detection conditions that were used in this study, are presented in **Table S1**. The  
182 incubation conditions and the detection conditions of these hydrolytic metabolites have been  
183 reported previously [29, 23, 24].

184 *2.3.2 Inhibition of hCE2-mediated Irinotecan hydrolysis by magnolol*

185 In brief, 194  $\mu\text{L}$  phosphate buffer (pH 7.4) was pre-mixed with 2  $\mu\text{L}$  HLM (200  $\mu\text{g}/\text{mL}$ ,  
186 final concentration) and 2  $\mu\text{L}$  magnolol at various concentrations. The mixtures were  
187 pre-incubated at 37  $^{\circ}\text{C}$  for 10 min, and then the hydrolytic reactions were initiated by adding  
188 irinotecan (5  $\mu\text{M}$ , final concentration). Following 50 min incubation at 37  $^{\circ}\text{C}$  in a shaking  
189 bath, all incubations were quenched by adding 200  $\mu\text{l}$  of ice-cold acetonitrile. After  
190 centrifuged at 20,000  $\times g$  for 20 min at 4  $^{\circ}\text{C}$ , 10  $\mu\text{L}$  of the supernatant was injected into the  
191 LC-FD system for further analysis. Both irinotecan and its metabolite SN38 were quantified  
192 by a liquid chromatography system (Shimadzu, Kyoto, Japan) coupled with a fluorescence  
193 detector, the method was modified according to a previous study [31]. Chromatographic  
194 separation of irinotecan and its metabolite SN-38 were performed using a Shim-pack ODS  
195 column (150 mm  $\times$  2.0 mm, 2  $\mu\text{m}$ , Shimadzu). Acetonitrile (A) and ammonium acetate (50  
196 mM, pH=4.0, B) were used as the mobile phase, and the gradient was as follow, 0.01-1.50  
197 min, 25% A; 1.50-6.00 min, 25-40% A; 6.00-8.00 min, 40-90% A; 8.00-12.00 min, 90% A;

198 12.00-12.50 min, 90-25% A; 12.50-15.00 min, 25% A. The column temperature was kept at  
199 40 °C and the flow rate was 0.6 mL/min.

#### 200 *2.4 Inhibition kinetic analyses*

201 To determine the inhibition constant ( $K_i$ ) and inhibition kinetic types of magnolol against  
202 hCEs, the inhibition kinetics of both hCE1 and hCE2 by magnolol were carefully investigated  
203 using varying concentrations of probe substrates in the presence of different concentrations of  
204 magnolol (inhibitor). The details for determining the inhibition constants have been reported  
205 previously [32-34].

#### 206 *2.5 Cell culture and fluorescence imaging analyses*

207 The inhibitory effects of magnolol on both hCE1 and hCE2 were also investigated in living  
208 HepG2 cells. To this end, HepG2 cells were cultured at 37 °C in 5% CO<sub>2</sub> in Modified Eagle's  
209 Medium (MEM) containing 0.1% antibiotic-antimycotic mix antibiotic, supplemented with 10%  
210 fetal bovine serum (FBS). For fluorescence imaging, HepG2 cells were seeded in 96-well  
211 plates (8000 cells / well) in complete medium and then incubated for 24 hours. Afterwards,  
212 the cells were washed twice with FBS-free culture medium and incubated in the medium  
213 containing magnolol (prepared in FBS-free at various concentrations) for 30 min at 37 °C  
214 under 5% CO<sub>2</sub>. To assess the intracellular hCE1 and hCE2 function, HepG2 cells were then  
215 co-incubated with BME (final concentration, 5 μM) or NCEN (final concentration, 10 μM)  
216 for another 30 min and 50 min, respectively. The living cells were imaged and analyzed using  
217 an ImageXpress® Micro Confocal High-Content Imaging system (Molecular Devices,  
218 Austria).

#### 219 *2.6 Prediction of herb-drug interaction potentials from in vitro data*

220 The potential risk of the metabolic interactions of magnolol on hCE1 was predicted *via*  
 221 evaluation of the changes in the area under the plasma concentration-time curve (AUC) in the  
 222 presence of magnolol. The  $AUC_{ratio}$  was predicted using the equation 1 [55].

$$AUC_{ratio} = \frac{1}{f_{hep} \left( \frac{1/E_h}{(1/E_h - 1)(1 + I/K_i) + 1} \right) + (1 - f_{hep})} \quad (1)$$

$$E_h = CL_{hep} / Q_h = \frac{1}{\frac{Q_h \times f_m \times K_m}{V_{max} \times MSP \times f_u} + 1} \quad (2)$$

225 Where  $f_{hep}$  is the percentage of hepatic clearance mediated by hCE1;  $E_h$  is the hepatic  
 226 extraction ratio;  $I$  is the maximum plasma concentration of magnolol, while  $K_i$  ( $\mu\text{M}$ ) is the  
 227 inhibitory constant of magnolol against hCE1;  $f_m$  is the fraction metabolized by hCE1;  $f_u$  is  
 228 the unbound fraction of magnolol;  $K_m$  ( $\mu\text{M}$ ) is the substrate affinity constant;  $V_{max}$   
 229 ( $\text{nmol} \cdot \text{min} \cdot \text{mg}$ ) is the maximum reaction velocity;  $Q_h$  ( $\text{ml}/\text{min}$ ) is the liver blood flow; and  
 230  $MSP$  ( $\text{mg}$ ) is the total microsomal proteins.

### 231 2.7 Molecular docking simulations of magnolol into hCEs

232 For docking simulations, Discovery Studio (BIOVIA Discovery Studio 2016, Dassault  
 233 Systèmes, San Diego, USA) was used to mimic the interactions of magnolol with both hCE1  
 234 and hCE2. The whole process for docking simulation was depicted previously [28].

### 235 2.8 Statistical analysis

236 All assayed were performed in triplicate and the results presented here were expressed as  
 237 mean  $\pm$  SD. The  $IC_{50}$  values were determined using nonlinear regression by GraphPad Prism  
 238 7.0 software (GraphPad Software, Inc., La Jolla, USA).

239

### 240 3. Results

#### 241 3.1 Assessments of human carboxylesterases inhibition by magnolol

242 Firstly, the inhibition potentials of magnolol on both hCE1 and hCE2 were screened using  
243 three inhibitor concentrations (1  $\mu\text{M}$ , 10  $\mu\text{M}$  and 100  $\mu\text{M}$ , final concentrations), while DME  
244 and FD were used as isoform-specific probes for hCE1 and hCE2 in HLM, respectively. As  
245 shown in **Fig. S1**, magnolol displayed potent inhibition of both hCE1-mediated DME  
246 hydrolysis and hCE2-mediated FD hydrolysis. Upon addition of magnolol (1  $\mu\text{M}$ ), the  
247 residual activities of hCE1 or hCE2 were less than 50%, suggesting that the  $\text{IC}_{50}$  values of  
248 magnolol against both hCE1-mediated DME hydrolysis and hCE2-mediated FD hydrolysis in  
249 HLM were less than 1  $\mu\text{M}$ . To quantify the half maximal inhibition concentration ( $\text{IC}_{50}$ ) of  
250 magnolol more accurately, the dose-response curves were plotted using different inhibitor  
251 concentrations. As shown in **Fig. 2A** and **Fig. 3A**, magnolol inhibited the catalytic activities  
252 of both hCE1 and hCE2 in a dose-dependent manner. The  $\text{IC}_{50}$  values of magnolol toward  
253 hCE1-mediated DME hydrolysis and hCE2-mediated FD hydrolysis in HLM were  
254 determined as 0.35  $\mu\text{M}$  and 0.90  $\mu\text{M}$ , respectively. These findings stimulated us to further  
255 investigate the mechanism of hCEs inhibition by magnolol, the most abundant natural  
256 constituent from *M. officinalis*.

#### 257 3.2 Kinetic analyses of human carboxylesterase 1 inhibition by magnolol

258 As shown in **Fig. S2**, inhibition of hCE1-mediated DME hydrolysis in HLM by magnolol  
259 was not time-dependent, suggesting that magnolol was a reversible inhibitor of hCE1 [35].  
260 Subsequently, the kinetics of hCE1 inhibition by magnolol was carefully studied using a  
261 panel of hCE1 substrates, including three optical substrates (DME, BMBT, BME) and a  
262 substrate drug (clopidogrel). As shown in **Fig. 2** and **Table 1**, magnolol exhibited significant

263 inhibitory effects toward hCE1-mediated hydrolysis of various substrates, all of them with  
264  $IC_{50}$  values below 1.2  $\mu\text{M}$ . The inhibition modes and the  $K_i$  values of magnolol of the  
265 hCE1-mediated hydrolysis inhibition were then carefully characterized in HLM, using these  
266 four different substrates. As shown in **Fig. 2** and **Fig. S11**, the inhibition kinetic plots clearly  
267 showed that magnolol inhibited hCE1-mediated hydrolysis of all the tested hCE1 substrates  
268 (including DME BMBT, BME and clopidogrel) in HLM *via* mixed inhibition mode, with the  
269  $K_i$  values ranging between 0.23  $\mu\text{M}$  and 1.36  $\mu\text{M}$  (**Table 1**). These findings indicate that  
270 magnolol is a potent hCE1 inhibitor for all the tested substrates.

### 271 *3.3 Kinetic analyses of human carboxylesterase 2 inhibition by magnolol*

272 Similarly, a time-dependent inhibition assay was also performed to ascertain the inhibition  
273 type of magnolol on hCE2. As shown in **Fig. S3**, prolonging the pre-incubation time did not  
274 affect the inhibition of hCE2-mediated FD hydrolysis in HLM by magnolol, suggesting that  
275 magnolol was a reversible inhibitor toward hCE2, too [35]. Subsequently, the inhibition  
276 kinetics of hCE2 by magnolol was investigated using three optical substrates for hCE2  
277 substrates, namely FD, 3-EBF, and NCEN, as well as the drug substrate irinotecan. The  $IC_{50}$   
278 values of magnolol in the hCE2-mediated hydrolysis of these substrates were 0.90  $\mu\text{M}$ , 2.74  
279  $\mu\text{M}$ , 10.21  $\mu\text{M}$  and 24.16  $\mu\text{M}$  for FD, 3-EBF, NCEN and irinotecan, respectively (**Table 1**).  
280 These findings revealed a rather large variability among the  $IC_{50}$  values of magnolol against  
281 the tested hCE2 substrates, in contrast to the situation with hCE1 (**Table 1**).

282 Kinetic analyses of hCE2 inhibition by magnolol using Lineweaver-Burk plots suggested  
283 that this natural compound was a mixed inhibitor against hCE2-mediated hydrolysis of all the  
284 tested hCE2 substrates (including FD, 3-EBF, NCEN and irinotecan) in HLM (**Fig. 3** and **Fig.**

285 **S11**). The large variability in  $IC_{50}$  values in the case of hCE2 was also reflected in the  $K_i$   
286 values for magnolol, when hCE2 substrates were used. The  $K_i$  values for the hydrolysis of FD,  
287 3-EBF, NCEN, and irinotecan were 1.02  $\mu$ M, 0.86  $\mu$ M, 17.13  $\mu$ M and 29.91  $\mu$ M, respectively.  
288 These results suggested that the inhibition of hCE2 by magnolol might be  
289 substrate-dependent.

### 290 *3.4 Inhibition of hCEs by magnolol in living cells*

291 Considering that hCEs were intracellular enzyme localized within the lumen of the  
292 endoplasmic reticulum, it was important to assay the inhibition potentials of magnolol, given  
293 on the outside, on intracellular hCEs. To this end, BME and NCEN were selected as highly  
294 specific fluorescent probe substrates for hCE1 and hCE2, respectively. This selection was due  
295 to the inherent advantages of these two fluorescent probe substrates, including high  
296 fluorescence quantum yield and good biocompatibility, as well as high chemical and  
297 photochemical stability [27, 24]. Prior to test the inhibitory effects of magnolol on  
298 intracellular hCEs in HepG2 cells, the cytotoxicity of magnolol towards HepG2 cells was  
299 assayed. As shown in **Fig S5**, magnolol exhibited weak cytotoxicity on HepG2 when the final  
300 concentration was lower than 60  $\mu$ M. But the HepG2 cells could be damaged at high dosage  
301 (100  $\mu$ M), with the cell viability of 37%. The inhibition assays were carried out and the  
302 results are shown in **Fig. S6**. Magnolol could inhibit intracellular hCE1-mediated BME  
303 hydrolysis and reduce the fluorescence intensity in the green channel (for the hydrolytic  
304 metabolite of BME) in living HepG2 cells in a dose-dependent manner. The  $IC_{50}$  value of this  
305 inhibition was measured and found to be 8.59  $\mu$ M. The inhibition of hCE2-mediated NCEN  
306 hydrolysis in living HepG2 cells by magnolol, on the other hand was weaker, exhibiting an

307  $IC_{50}$  value higher than 60  $\mu$ M, the highest concentration of magnolol that was used in the  
308 assay (**Fig. S7**). These findings suggest that magnolol is cell membrane permeable and  
309 capable of inhibiting the endogenous hCE1 in living cells.

### 310 *3.5 Docking simulations of magnolol in hCE1 and hCE2*

311 A different approach for further understanding the interactions of magnolol with hCEs was  
312 docking simulations. As shown in **Fig. 4**, magnolol could be well-docked into hCE1 at two  
313 distinct ligand-binding sites, one located inside the catalytic cavity and another on the  
314 regulatory domain (Z site). This finding suggests that magnolol could bind on hCE1 at two  
315 distinct ligand-binding sites, one of which overlaps and competes with DME for its binding  
316 site within the catalytic cavity of hCE1, while the other magnolol-binding site is located on  
317 the regulatory domain that is situated far away from the catalytic triad of the enzyme. Hence,  
318 the mixed-type inhibition of magnolol in hCE1 probably resulted from competitive inhibition  
319 by binding at the catalytic cavity and non-competitive inhibition from binding at the  
320 regulatory domain.

321 The key residues for the interactions between magnolol and hCE1 were also analyzed by  
322 docking simulations. As depicted in **Fig. 4** and **Fig. S8**, magnolol could interact with residues  
323 around the catalytic cavity of hCE1 mainly *via* hydrophobic interactions, while at the  
324 regulatory domain of hCE1 magnolol would mainly bind through hydrogen bonding and  
325 hydrophobic interactions. As a result, the docking simulations of magnolol on both the active  
326 site and the Z site in the best binding conformations yielded the lowest binding free energies  
327 (-95.82 kcal/mol for magnolol binding at the catalytic site of hCE1, and -90.06 kcal/mol for  
328 binding at the Z site).



329 As depicted in **Fig. 5**, magnolol could also be well-docked into both the catalytic cavity  
330 and the regulatory domain (Z site) of hCE2, suggesting that magnolol could compete with FD  
331 for an overlapping site in the catalytic cavity. The latter and the 2<sup>nd</sup> binding site at the  
332 regulatory domain, far away from the catalytic triad of hCE2, could well explain the  
333 mixed-type kinetics of magnolol in hCE2 inhibition. As shown in **Fig. 5** and **Fig. S9**,  
334 magnolol appears to be tightly bind at residues around the catalytic cavity of hCE2,  
335 predominantly *via* hydrophobic interactions, while the binding energy of the best binding  
336 mode (magnolol on the active site of hCE2) was estimated as -85.92 kcal/mol. It was also  
337 found that magnolol could strongly bind at the regulatory domain of hCE2 through both  
338 hydrogen bonding and hydrophobic interactions. The binding energy of the best binding  
339 mode of magnolol on the Z site of hCE2 was as low as -109.99 kcal/mol. It thus appears that  
340 the docking results agree with the inhibition kinetics results, for both hCE1 and hCE2  
341 inhibition by magnolol.

### 342 *3.6 Quantitative prediction of magnolol-associated HDI risks via hCE1 inhibition*

343 Considering that magnolol could inhibit intracellular hCE1 in living cells and its inhibition  
344 potency was really strong, it was necessary to evaluate the potential risks of magnolol *via*  
345 hCE1 inhibition. In this case, the magnitudes of the metabolic interactions between magnolol  
346 and hCE1 substrate drug was predicted by estimating the changes in the AUCs of the hCE1  
347 substrate drugs (or the drugs predominantly metabolized by hCE1) co-administrated with  
348 magnolol-containing marketed products. The AUC ratios were calculated based on a series of  
349 available pharmacokinetic data and inhibition constants, including the hepatic extraction ratio  
350 ( $E_h$ ), the percentage of hepatic clearance mediated by hCE1 relative to the total clearance of

351 the substrates ( $f_{hep}$ ), the  $K_i$  values for magnolol against hCE1 and the predicted maximum  
352 concentration of magnolol in human plasma ( $C_{max}$ ). As shown in **Table S3**, magnolol might  
353 increase the AUCs of the clopidogrel by 28%-142% when clopidogrel was co-administrated  
354 with magnolol-containing products. This finding implied that magnolol might modulate the  
355 pharmacokinetic behaviors of the ester-bearing drugs that predominantly metabolized by  
356 hCE1, such as clopidogrel.

357

#### 358 **4. Discussion**

359 Over the past decade, increasing evidence has demonstrated that human carboxylesterases  
360 (hCEs) play crucial roles in both endogenous and xenobiotic metabolism [20, 22, 36]. The  
361 biological roles of hCEs have raised great interest in the discovery of potent hCEs modulators  
362 that can be used to regulate lipid metabolism or to improve the treatment outcomes of ester  
363 drugs [37]. In recent years, many groups have tried to identify potent inhibitors of hCEs from  
364 edible herbs, since most edible herbs have displayed good safety profiles during long history  
365 of use in medical applications. Our preliminary studies have found that crude extracts of  
366 some herbs (such as *Fructus Psoraleae* and *Magnolia officinalis*) strongly inhibit the activity  
367 of hCEs [38]. Unfortunately, the major constituents of *Fructus Psoraleae* can trigger  
368 hyperbilirubinemia and liver injury *via* strong inhibition of human  
369 UDP-glucuronosyltransferase 1A1 [39]. Therefore, it is of great importance to find more  
370 readily available ingredients or natural compounds with good safety profiles as hCEs  
371 inhibitors [32, 40, 56]. In the present study, the results clearly demonstrate that magnolol (the  
372 most abundant constitute in *Magnolia officinalis*) displays potent inhibition on

373 hCE1-mediated hydrolysis of a panel of substrates. Magnolol also exhibits strong to moderate  
374 inhibition of hCE2-mediated hydrolysis of various substrates in HLM. The initial  
375 observations prompted us to deepen and extend our investigation on the inhibition  
376 mechanism of magnolol against both hCEs.

377 As an abundant drug-metabolizing enzyme in the liver, hCE1 can effectively hydrolyse a  
378 variety of ester drugs, as well as prodrugs with ester bonds or amide bonds, including  
379 clopidogrel, temopril, midazolam, oseltamivir and enalapril [12, 13]. Thus, co-administration  
380 of one of the above listed hCE1 substrate drugs with magnolol-containing products, may  
381 trigger clinically relevant drug/herb-drug interactions [17]. Notably, inhibition of hCE1 is a  
382 double-edged sword for patients administrated with hCE1-substrate drugs. Strong inhibition  
383 of hepatic hCE1 may slow down the hydrolytic rates of hCE1 substrates *in vivo*, which may  
384 affect the pharmacokinetic properties of co-administrated ester drugs and thus bring  
385 beneficial effects (such as enhancement of efficacy) or unbeneficial effects (such as herb-drug  
386 interactions). For example, hCE1 catalyses oseltamivir hydrolysis to form the active  
387 metabolite oseltamivir carboxylate, thus inhibition of hCE1 may result in decreased plasma  
388 exposure of oseltamivir carboxylate and reduce efficacy of this hCE1-substrate drug [41]. By  
389 contrast, clopidogrel, one of the most frequently prescribed antiplatelet agents, can be rapidly  
390 hydrolysed to an inactive metabolite by hepatic hCE1, whereas only about 15% of this ester  
391 drug is activated by CYPs to form 2-oxo-clopidogrel, followed by conversion to the active  
392 metabolite [42]. Dysfunction or inhibition of hCE1 may partially block the hydrolysis of  
393 clopidogrel and accelerated the formation rate of the active metabolite *via* the CYP-mediated  
394 pathway [14]. Thus, magnolol-containing products or MBEs could modulate the efficacy of

395 clopidogrel in the clinic. This result of our study, reasonable use magnolol-containing  
396 products, may be helpful for clinical pharmacists.

397 In addition to the involvement of xenobiotic metabolism, hCE1 also participates in the  
398 hydrolytic metabolism of some key endogenous esters, such as cholesterol esters and  
399 triglycerides [43]. This indicates that hCE1 inhibitors (such as magnolol) may regulate lipid  
400 metabolism and cholesterol homeostasis *via* hCE1 inhibition. Recently, Dominguez et al has  
401 found that the levels and enzymatic activities of hCE1 in subcutaneous adipose tissue and  
402 visceral adipose tissue from obese and type 2 diabetic patients are much higher than that of  
403 health individuals, while treatment with hCE1 inhibitors may benefit the patients with obesity  
404 and type 2 diabetes through improving metabolic features [22]. It should be noted that  
405 magnolol has been found to have anti-diabetic effects and other beneficial effects on a panel  
406 of metabolic diseases. For example, a recent investigation has demonstrated that oral  
407 administration of this compound to type 2 diabetic rats could reduce fasting blood glucose  
408 and plasma insulin levels, as well as induce glucose uptake in adipocytes [44]. Interestingly,  
409 in the present study, we found that magnolol is a potent and cell permeable inhibitor of hCE1,  
410 it could strongly inhibit intracellular hCE1 in living cells. This finding indicates that  
411 magnolol may inhibit some key intracellular hCE1-mediated endogenous esters hydrolysis,  
412 which in turn alleviate the metabolic disorders of type 2 diabetes. At least, intracellular hCE1  
413 may be one of the targets of magnolol for the prevention and treatment of diabetes or other  
414 metabolic diseases.

415 Considering that hCE2 plays a key role in the hydrolysis of some important ester drugs,  
416 such as irinotecan and capecitabine [45, 46], the inhibition potentials of magnolol on hCE2

417 was also investigated in HLM and living cells. The results demonstrate that magnolol  
418 displays strong inhibition on hCE2-mediated hydrolysis of FD and 3-EBF, but the inhibition  
419 of hCE2-mediated hydrolysis of NCEN and irinotecan was moderate (**Table 1**). The  
420 substrate-dependent inhibition of hCE2-mediated hydrolysis reactions by magnolol could be  
421 partially explained by the larger catalytic cavity of this enzyme. As shown in **Fig. S10**, the  
422 volume of the catalytic cavity of hCE2 is about 2-fold larger than that of hCE1, which  
423 suggests that the catalytic cavity of hCE2 can simultaneously accommodate more than one  
424 small molecule ligands. Furthermore, evidence from X-ray crystal structure of hCE1 revealed  
425 that under physiological conditions hCE1 exists as a mixture of monomeric and trimeric, as  
426 well as hexameric forms [36]. By contrast, hCE2 exists as a monomer. Thus, it is conceivable  
427 that the conformation of hCE2 could be easily changed by binding of ligands but the changes  
428 in the conformation of hCE1 in such a way is relatively difficult, owing to the major forms of  
429 hCE1 are trimer or hexamer, which may partially block the free access of the ligands.

430 Taking into account that hCE2 is an intracellular target that is localized in the lumen of ER,  
431 it is necessary to ascertain the inhibition potential of magnolol on intracellular hCE2. In these  
432 cases, we use NCEN (a fluorescent probe substrate for hCE2) to replace irinotecan in order to  
433 assay the inhibitory effects of magnolol on hCE2 inside living cells. This is because both  
434 NCEN and its hydrolytic metabolite exhibit excellent optical properties [24], as well as  
435 similar inhibition tendency as the hCE2 substrate drug irinotecan. Notably, the results  
436 demonstrate that magnolol hardly inhibits hCE2-mediated NCEN hydrolysis in living HepG2  
437 cells. These findings suggest that the inhibition potency of magnolol on intracellular hCE2 is  
438 relatively weak in living HepG2 cells, which may partially be attributed to the metabolic

439 clearance of magnolol in HepG2 cells [47].

440 Although magnolol displayed strong inhibition of hCE1, its potency and selectivity is not  
441 so high. Therefore, it is desirable to further develop more potent hCE1 inhibitors using this  
442 natural compound as lead compound. As mentioned above, the content of magnolol in  
443 *Magnolia officinalis* is very high [4], the medicinal chemists can easily get this natural  
444 compound from this herb and then to semi-synthesize a variety of structurally diverse  
445 magnolol derivatives for systematic pharmacological and toxicological studies. To develop a  
446 potent and highly specific hCE1 inhibitor, it is necessary to explore the structure-activity  
447 relationships of magnolol derivatives as hCE1 inhibitors, as well as to assay their specificity  
448 towards hCE1 over other serine hydrolases. Considering that the crystal structure and the  
449 catalytic triad of hCE1 have been reported [48], hCE1 inhibitors could be rationally designed  
450 and developed with the help of computer-assisted virtual screening and design. Considering  
451 that magnolol can be readily metabolized by hepatic drug metabolizing enzyme [47],  
452 attention should be paid to further optimization of the metabolic stability of magnolol  
453 derivatives during lead to candidate optimization. In addition, in the future, the medicinal  
454 chemists could consider designing dual inhibitors against both hCE1 and other target(s) for  
455 the treatment of metabolic diseases [49, 50]. All these investigations will be very helpful for  
456 the discovery of novel efficacious hCE1 inhibitors for potential medical applications.

457

## 458 **5. Conclusion**

459 In summary, the inhibitory effects of magnolol on human carboxylesterases (hCEs), key  
460 enzymes participating in the hydrolytic metabolism of a wide range of endogenous and

461 xenobiotic esters, were carefully investigated using a panel of hCEs substrates including  
462 optical substrates and substrate drugs. Our results demonstrated that magnolol was a strong  
463 inhibitor of hCE1-mediated hydrolysis of all the tested substrates. By contrast, magnolol  
464 displayed strong inhibition of hCE2-mediated hydrolysis of FD and 3-EBF, but moderate  
465 inhibition of NCEN and irinotecan hydrolysis. The inhibition mechanism of magnolol against  
466 both hCE1 and hCE2 were carefully investigated by a panel of kinetic analyses and docking  
467 simulations, the results showed that magnolol could tightly bind on hCE1 or hCE2 at both the  
468 catalytic cavity and the regulatory domain, which was consistent with the experimental data  
469 in which this compound functions as a potent hCEs inhibitor *via* mixed-inhibition manner.  
470 Further investigation demonstrated that magnolol could also strongly inhibit intracellular  
471 hCE1 but hardly inhibit intracellular hCE2-mediated NCEN hydrolysis. All these findings  
472 provided new insights into the interactions between magnolol and hCEs, which was very  
473 useful for avoiding deleterious interactions *via* modulating the pharmacokinetic behaviors of  
474 hCEs-substrate drugs. Additionally, these findings clearly suggested that magnolol could be  
475 used as a good lead compound for the development of more efficacious hCEs inhibitors with  
476 good safety profile.

477

#### 478 **Declaration of interest**

479 The authors have no conflicts of interests.

480

#### 481 **Acknowledgements**

482 This work was supported by the National Key Research and Development Program of

483 China (2016YFC1303900, 2017YFC1700200, 2017YFC1702000), the NSF of China  
484 (81773687, 81703604, 81803489), Program of Shanghai Academic/Technology Research  
485 Leader (18XD1403600), Shuguang Program (18SG40) supported by Shanghai Education  
486 Development Foundation and Shanghai Municipal Education Commission, the Innovative  
487 Entrepreneurship Program of High-level Talents in Dalian (2016RQ025 & 2017RQ121), and  
488 China Postdoctoral Science Foundation (2017M621520 and 2018T110406).

489

#### 490 **Appendix A. Supplementary material**

491 Supplementary data associated with this article can be found, in the online version, at [http:](http://)

492

#### 493 **References**

494 [1] S. X. Yu, R. Y. Yan, R. X. Liang, W. Wang, B. Yang, Bioactive polar compounds from stem bark of  
495 *Magnolia officinalis*, *Fitoterapia*. 83 (2012) 356-361.

496 [2] K. Iwasaki, Q. Wang, H. Seki, K. Satoh, A. Takeda, H. Arai, H. Sasaki, The effects of the traditional  
497 Chinese medicine, “Banxia Houpo Tang (Hange-Koboku To)” on the swallowing reflex in Parkinson's  
498 disease, *Phytomedicine*. 7 (2000) 259-263.

499 [3] M. Fukushima, Profiles of effects of traditional oriental herbal medicines on central nervous systems  
500 in humans-assessment of saiboku-to and saiko-ka-ryukotsu-borei-to using EEG and pharmacokinetics of  
501 herbal medicine-derived ingredients as indices, *Seishin Shinkeigaku Zasshi*. 99 (1997) 355-369.

502 [4] EPCNF (European Parliament Concerning Novel Foods and Novel Food Ingredients), Application for  
503 the Approval of Magnolia Bark Supercritical Carbon Dioxide Extract (MBSE) from *Magnolia officinalis*.  
504 (2009) The William Wrigley Jr. Company, Chicago.

505 [5] Z. Liu, X. Zhang, W. Cui, X. Zhang, N. Li, J. Chen, A. W. Wong, A. Roberts, Evaluation of short-term  
506 and subchronic toxicity of magnolia bark extract in rats, *Regul. Toxicol. Pharmacol.* 49 (2007) 160-171.

507 [6] S. B. Kim, H. E. Kang, H. J. Cho, Y. S. Kim, S. J. Chung, I. S. Yoon, D. D. Kim, Metabolic  
508 interactions of magnolol with cytochrome P450 enzymes: uncompetitive inhibition of CYP1A and



- 509 competitive inhibition of CYP2C, *Drug Dev Ind Pharm.* 42 (2016) 263-269.
- 510 [7] L. L. Zhu, G. B. Ge, Y. Liu, G. Y. He, S. C. Liang, Z. Z. Fang, P. P. Dong, Y. F. Cao, L. Yang, Potent  
511 and selective inhibition of magnolol on catalytic activities of UGT1A7 and 1A9, *Xenobiotica.* 42 (2012)  
512 1001-1008.
- 513 [8] M. Greenberg, P. Urnezis, M. Tian, Compressed mints and chewing gum containing magnolia bark  
514 extract are effective against bacteria responsible for oral malodor, *J Agric Food Chem.* 55 (2007)  
515 9465-9469.
- 516 [9] T. Satoh, M. Hosokawa, Structure, function and regulation of carboxylesterases, *Chem. Biol. Interact.*  
517 162 (2006) 195-211.
- 518 [10] S. P. Sanghani, P. C. Sanghani, M. A. Schiel, W. F. Bosron, Human Carboxylesterases: An Update on  
519 CES1, CES2 and CES3, *Protein Pept. Lett.* 16 (2009) 1207-1214.
- 520 [11] T. Fukami, T. Yokoi, The emerging role of human esterases, *Drug Metab. Pharmacokinet.* 27 (2012)  
521 466-477.
- 522 [12] M. Hosokawa, Structure and catalytic properties of carboxylesterase isozymes involved in metabolic  
523 activation of prodrugs, *Molecules.* 13 (2008) 412-431.
- 524 [13] M. J. Hatfield, R. A. Umans, J. L. Hyatt, C. C. Edwards, M. Wierdl, L. Tsurkan, M. R. Taylor, P. M.  
525 Potter, Carboxylesterases: General detoxifying enzymes, *Chem. Biol. Interact.* 259 (2016) 327-331.
- 526 [14] D. Danielak, M. Karażniewicz-Łada, A. Komosa, P. Burchardt, M. Lesiak, L. Kruszyna, A.  
527 Graczyk-Szuster, F. Glowka, Influence of genetic co-factors on the population pharmacokinetic model for  
528 clopidogrel and its active thiol metabolite, *Eur. J. Clin. Pharmacol.* 73 (2017) 1623-1632.
- 529 [15] J. S. Hulot, A. Bura, E. Villard, M. Azizi, V. Remones, C. Goyenvalle, M. Aiach, P. Lechat, P.  
530 Gaussem, Cytochrome P450 2C19 loss-of-function polymorphism is a major determinant of clopidogrel  
531 responsiveness in healthy subjects, *Blood.* 108 (2006) 2244-2247.
- 532 [16] L. D. Hicks, J. L. Hyatt, S. Stoddard, L. Tsurkan, C. C. Edwards, R. M. Wadkins, P. M. Potter,  
533 Improved, selective, human intestinal carboxylesterase inhibitors designed to modulate  
534 7-ethyl-10-[4-(1-piperidino)-1-piperidino]carbonyloxycamptothecin (Irinotecan; CPT-11) toxicity, *J. Med.*  
535 *Chem.* 52 (2009) 3742-3752.
- 536 [17] J. N. Li, Y. F. Cao, R. R. He, G. B. Ge, B. Guo, J. J. Wu, Evidence for Shikonin acting as an active  
537 inhibitor of human carboxylesterases 2: Implications for herb-drug combination, *Phytother Res.* 32 (2018)  
538 1311-1319.

- 539 [18] S. P. Sanghani, S. K. Quinney, T. B. Fredenburg, Z. J. Sun, W. I. Davis, D. J. Murry, O. W.  
540 Cummings, D. E. Seitz, W. F. Bosron, Carboxylesterases expressed in human colon tumor tissue and their  
541 role in CPT-11 hydrolysis, *Clinical Cancer Research*. 9 (2003) 4983-4991.
- 542 [19] Y. G. li, J. Hou, S. Y. Li, Z. M. Liu, X. Lv, J. Ning, G. B. Ge, J. Y. Ren, L. Yang, Fructus Psoraleae  
543 (Bu-gu-zhi) contains natural compounds with potent inhibitory effects towards human carboxylesterase 2,  
544 *Fitoterapia*. 101 (2015) 99-106.
- 545 [20] A. D. Quiroga, L. Li, M. Trötz Müller, R. Nelson, S. D. Proctor, H. Köfeler, R. Lehner, Deficiency of  
546 Carboxylesterase 1/Esterase-x Results in Obesity, Hepatic Steatosis, and Hyperlipidemia, *Hepatology*. 56  
547 (2012) 2188-2198.
- 548 [21] S. Nagashima, H. Yagyu, N. Takahashi, T. Kurashina, M. Takahashi, T. Tsuchita, F. Tazoe, X. L.  
549 Wang, T. Bayasgalan, N. Sato, K. Okada, S. Nagasaka, T. Gotoh, M. Kojima, M. Hyodo, H. Horie, Y.  
550 Hosoya, M. Okada, Y. Yasuda, H. Fujiwara, M. Ohwada, S. Iwamoto, M. Suzuki, H. Nagai, S. Ishibashi,  
551 Depot-specific expression of lipolytic genes in human adipose tissues-association among CES1  
552 expression, triglyceride lipase activity and adiposity, *J Atheroscler Thromb*. 18 (2011) 190-199.
- 553 [22] E. Dominguez, A. Galmozzi, J. W. Chang, K. L. Hsu, J. Pawlak, W. Li, Integrated phenotypic and  
554 activity-based profiling links ces3 to obesity and diabetes, *Nat. Chem. Biol*. 10 (2014) 113-121.
- 555 [23] L. Feng, Z. M. Liu, J. Hou, X. Lv, J. Ning, G. B. Ge, J. N. Cui, L. Yang, A highly selective  
556 fluorescent ES IPT probe for the detection of Human carboxylesterase 2 and its biological applications.  
557 *Biosens Bioelectron*, 65 (2015) 9-15.
- 558 [24] Q. Jin, L. Feng, D. D. Wang, Z. R. Dai, P. Wang, L. W. Zou, Z. H. Liu, J. Y. Wang, Y. Yu, G. B. Ge, J.  
559 N. Cui, L. Yang, A two-photon ratiometric fluorescent probe for imaging carboxylesterase 2 in living cells  
560 and tissues, *ACS Appl. Mater. Interfaces* 7 (2015) 24874-24881.
- 561 [25] D. D. Wang, J. Qiang, H. Jie, F. Lei, L. Na, S. Y. Li, Highly sensitive and selective detection of  
562 human carboxylesterase 1 activity by liquid chromatography with fluorescence detection, *J. Chromatogr.*  
563 *B*. 1008 (2016) 212-218.
- 564 [26] D. D. Wang, Q. Jin, L. W. Zou, J. Hou, X. Lv, W. Lei, A bioluminescent sensor for highly selective  
565 and sensitive detection of human carboxylesterase 1 in complex biological samples, *Chem. Commun*. 52  
566 (2016) 3183-3186.
- 567 [27] L. L. Ding, Z. H. Tian, J. Hou, T. Y. Dou, Q. Jin, D. D. Wang, L. W. Zou, Y. D. Zhu, Y. Q. Song, J. N.  
568 Cui, G. B. Ge, Sensing carboxylesterase 1 in living systems by a practical and isoform-specific

- 569 fluorescent probe, *Chin. Chem. Lett.* 30 (2019) 558-562.
- 570 [28] Y. Q. Wang, Z. M. Weng, T. Y. Dou, J. Hou, D. D. Wang, L. L. Ding, L. W. Zou, Y. Yu, J. Chen, H.  
571 Tang, G. B. Ge, Nevadensin is a naturally occurring selective inhibitor of human carboxylesterase 1, *Int J*  
572 *Biol Macromol.* 120 (2018) 1944-1954.
- 573 [29] J. Wang, E. T. Williams, J. Bourgea, Y. N. Wong, C. J. Patten, Characterization of recombinant  
574 human carboxylesterases: fluorescein diacetate as a probe substrate for human carboxylesterase 2, *Drug*  
575 *Metab. Dispos.* 39 (2011) 1329-1333.
- 576 [30] D. Abigerges, J. P. Armand, G. G. Chabot, Costa. L. Da, E. Fadel, C. Cote, P. Hérait, D. Gandia,  
577 Irinotecan (CPT-11) high-dose escalation using intensive high-dose loperamide to control diarrhea, *J Natl*  
578 *Cancer Inst.* 86 (1994) 446-449.
- 579 [31] T. F. Shao, Y. T. Zheng, J. L. Xu, W. M. Cai, An analytical method built for irinotecan and its active  
580 metabolite sn-38 in human plasma using hplc-fld, *Chinese Journal of Hospital Pharmacy.* 32 (2012)  
581 17-19.
- 582 [32] Z. M. Weng, G. B. Ge, T. Y. Dou, P. Wang, P. K. Liu, X. H. Tian, N. Qiao, Y. Yu, L.W. Zou, Q. Zhou,  
583 W. D. Zhang, J. Hou, Characterization and structure-activity relationship studies of flavonoids as  
584 inhibitors against human carboxylesterase 2, *Bioorg. Chem.* 77 (2018) 320-329.
- 585 [33] X. Y. Liu, X. Lv, P. Wang, C. Z. Ai, Q. H. Zhou, M. Finel, B. Fan, Y. F. Cao, H. Tang, G. B. Ge,  
586 Inhibition of UGT1A1 by natural and synthetic flavonoids, *Int. J. Biol. Macromol.* 126 (2018) 653-661.
- 587 [34] X. Lv, J. B. Zhang, X. X. Wang, W. Z. Hu, Y. S. Shi, S.W. Liu, D. C. Hao, W. D. Zhang, G. B. Ge, J.  
588 Hou, L. Yang, Amentoflavone is a potent broad-spectrum inhibitor of human  
589 UDP-glucuronosyltransferases, *Chem. Biol. Interact.* 284 (2018) 48-55.
- 590 [35] Z. Chen, S. Zhang, N. Long, L. Lin, T. Chen, F. Zhang, An improved substrate cocktail for assessing  
591 direct inhibition and time-dependent inhibition of multiple cytochrome P450s. *Acta Pharmacol. Sin.* 37  
592 (2016) 708-718.
- 593 [36] D. D. Wang, L. W. Zou, Q. Jin, J. Hou, G. B. Ge, L. Yang, Human carboxylesterases: a  
594 comprehensive review, *Acta Pharm Sin B.* 8 (2018) 699-712.
- 595 [37] M. A. Ruby, J. Massart, D. M. Hunerdosse, M. Schönke, J. C. Correia, S. M. Louie, J. L. Ruas, E.  
596 Näslund, D. K. Nomura, J. R. Zierath, Human Carboxylesterase 2 Reverses Obesity-Induced  
597 Diacylglycerol Accumulation and Glucose Intolerance, *Cell Rep.* 218 (2017) 636-646.
- 598 [38] D. X. Sun, G. B. Ge, P. P. Dong, Y. F. Cao, Z. W. Fu, R. X. Ran, Inhibition behavior of fructus

- 599 psoraleae's ingredients towards human carboxylesterase 1 (hCES1), *Xenobiotica*. 46 (2016) 503-510.
- 600 [39] X. X. Wang, X. Lv, S. Y. Li, J. Hou, J. Ning, J. Y. Wang, Identification and characterization of  
601 naturally occurring inhibitors against UDP-glucuronosyltransferase 1A1 in fructus psoraleae (Bu-gu-zhi),  
602 *Toxicol. Appl. Pharmacol.* 289 (2015) 70-78.
- 603 [40] L. W. Zou, Q. Jin, D. D. Wang, Q. K. Qian, D. C. Hao, G. B. Ge, L. Yang, Carboxylesterase  
604 inhibitors: an update, *Curr. Med. Chem.* 25 (2018) 1627-1649.
- 605 [41] R. B. Parker, Z. Y. Hu, B. Meibohm, S. C. Laizure, Effects of alcohol on human carboxylesterase  
606 drug metabolism, *Clin Pharmacokinet.* 54 (2015) 627-638.
- 607 [42] H. J. Zhu, X. W. Wang, B. E. Gawronski, B. J. Brinda, D. J. Angiolillo, J. S. Markowitz,  
608 Carboxylesterase 1 as a Determinant of Clopidogrel Metabolism and Activation, *J Pharmacol Exp Ther.*  
609 344 (2013) 665-72.
- 610 [43] J. Lian, R. Nelson, R. Lehner, Carboxylesterases in lipid metabolism: from mouse to human, *Protein*  
611 *Cell.* 9 (2018) 178-195.
- 612 [44] M. Poivre, P. Duez, Biological activity and toxicity of the Chinese herb *Magnolia officinalis* Rehder  
613 & E. Wilson (Houpo) and its constituents, *Journal of Zhejiang University-SCIENCE B.* 18 (2017)  
614 194-214.
- 615 [45] P. M. Potter, J. S. Wolverson, C. L. Morton, M. Wierdl, M. K. Danks, Cellular localization domains  
616 of a rabbit and a human carboxylesterase: influence on irinotecan (CPT-11) metabolism by the rabbit  
617 enzyme, *Cancer Res.* 58 (1998) 3627-3632.
- 618 [46] S. K. Quinney, S. P. Sanghani, W. I. Davis, T. D. Hurley, Z. Sun, D. J. Murry, W. F. Bosron,  
619 Hydrolysis of capecitabine to 5'-deoxy-5-fluorocytidine by human carboxylesterases and inhibition by  
620 loperamide, *J. Pharmacol. Exp. Ther.* 313 (2005) 1011-1016.
- 621 [47] L. L. Zhu, G. B. Ge, H. B. Zhang, H. X. Liu, G. Y. He, S. C. Liang, Y. Y. Zhang, Z. Z. Fang, P. P.  
622 Dong, M. Finel, L. Yang, Characterization of hepatic and intestinal glucuronidation of magnolol:  
623 application of the relative activity factor approach to decipher the contributions of multiple  
624 UDP-glucuronosyltransferase isoforms, *Drug Metab Dispos.* 40 (2012) 529-538.
- 625 [48] S. Bencharit, C. L. Morton, J. L. Hyatt, P. Kuhn, M. K. Danks, P. M. Potter, M. R. Redinbo, (2003).  
626 Crystal structure of human carboxylesterase 1 complexed with the alzheimer's drug tacrine: from binding  
627 promiscuity to selective inhibition, *Chem. Biol.* 10 (2003) 341-349.
- 628 [49] K. Tang, I. Konczak, J. Zhao, Phenolic compounds of the australian native herb *prostanthera*

- 629 rotundifolia and their biological activities, *Food Chem.* 233 (2017) 530-539.
- 630 [50] L. W. Zou, Y. G. Li, P. Wang, K. Zhou, J. Hou, Q. Jin, Design, synthesis, and structure-activity  
631 relationship study of glycyrrhetic acid derivatives as potent and selective inhibitors against human  
632 carboxylesterase 2, *Eur. J. Med. Chem.* 112 (2016) 280-288.
- 633 [51] R. P. Austin, P. Barton, S. L. Cockroft, M. C. Wenlock, R. J. Riley, The influence of nonspecific  
634 microsomal binding on apparent intrinsic clearance, and its prediction from physicochemical properties,  
635 *Drug Metab Dispos.* 30 (2002) 1497.
- 636 [52] M. Tang, M. Mukundan, J. Yang, N. Charpentier, E. L. LeCluyse, C. Black, D. Yang, D. Shi & B.  
637 Yan, Antiplatelet agents aspirin and clopidogrel are hydrolyzed by distinct carboxylesterases, and  
638 clopidogrel is transesterificated in the presence of ethyl alcohol, *J Pharmacol Exp Ther.* 319 (2006)  
639 1467-1476.
- 640 [53] G. Campus, M. G. Cagetti, F. Cocco, S. Sale, G. Sacco, L. Strohmenger & P. Lingstrom, Effect of a  
641 sugar-free chewing gum containing magnolia bark extract on different variables related to caries and  
642 gingivitis: a randomized controlled intervention trial, *Caries Res.* 45 (2011) 393-399.
- 643 [54] J. Feldschuh & Y. Enson, Prediction of the normal blood volume. Relation of blood volume to body  
644 habitus, *Circulation.* 56 (1977) 605-612.
- 645 [55] B. J. Kirby & J. D. Unadkat, Impact of ignoring extraction ratio when predicting drug-drug  
646 interactions, fraction metabolized, and intestinal first-pass contribution, *Drug Metab. Dispos. Biol. Fate*  
647 *Chem.* 38 (2010) 1926-1933.
- 648 [56] D. D. Wang, L. W. Zou, Q. Jin, J. Hou, G. B. Ge, L. Yang, Recent progress in the discovery of  
649 natural inhibitors against human carboxylesterases, *Fitoterapia.* 117 (2017) 84-95.
- 650

651

652

**Table 1.** The inhibition parameters and inhibition modes of magnolol against hCEs.

Target enzyme	Enzyme source	Substrate	IC <sub>50</sub> (μM)	<i>f<sub>u</sub></i>	<i>f<sub>u</sub></i> *IC <sub>50</sub> (μM)	<i>K<sub>i</sub></i> (μM)	Inhibition mode	Goodness of fit (R <sup>2</sup> )
hCE1	HLM	DME	0.35±0.01	0.98	0.34	0.34	Mixed	0.99
hCE1	HLM	BMBT	0.70±0.05	1.00	0.70	0.52	Mixed	0.99
hCE1	HLM	BME	0.21±0.02	0.96	0.20	0.23	Mixed	0.99
hCE1	HLM	Clopidogrel	1.14±0.10	0.50	0.57	1.36	Mixed	0.92
hCE2	HLM	FD	0.90±0.04	0.96	0.86	1.02	Mixed	0.97
hCE2	HLM	3-EBF	2.74±0.24	0.84	2.30	0.86	Mixed	0.99
hCE2	HLM	NCEN	10.21±3.15	0.84	8.58	17.13	Mixed	0.97
hCE2	HLM	Irinotecan	24.16±5.21	0.20	4.83	29.91	Mixed	0.95

653 Note. Estimate the in vitro fraction unbound from drug's properties. Equations published by Austin  
654 are being used for this calculation. For microsomes: % unbound =  
655  $100/[MicrosConc*[10^{[0.56*\log D/P-1.41]}]+1]$  [51]; logP value of magnolol was set to 4.83.

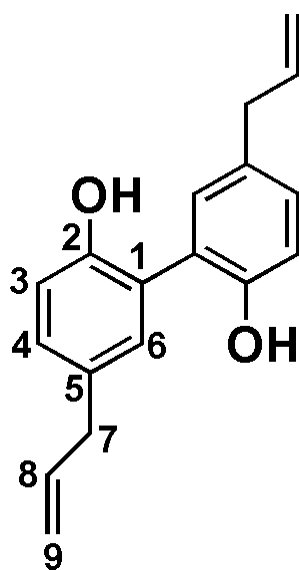


**Fig. 1.** The chemical structure of magnolol

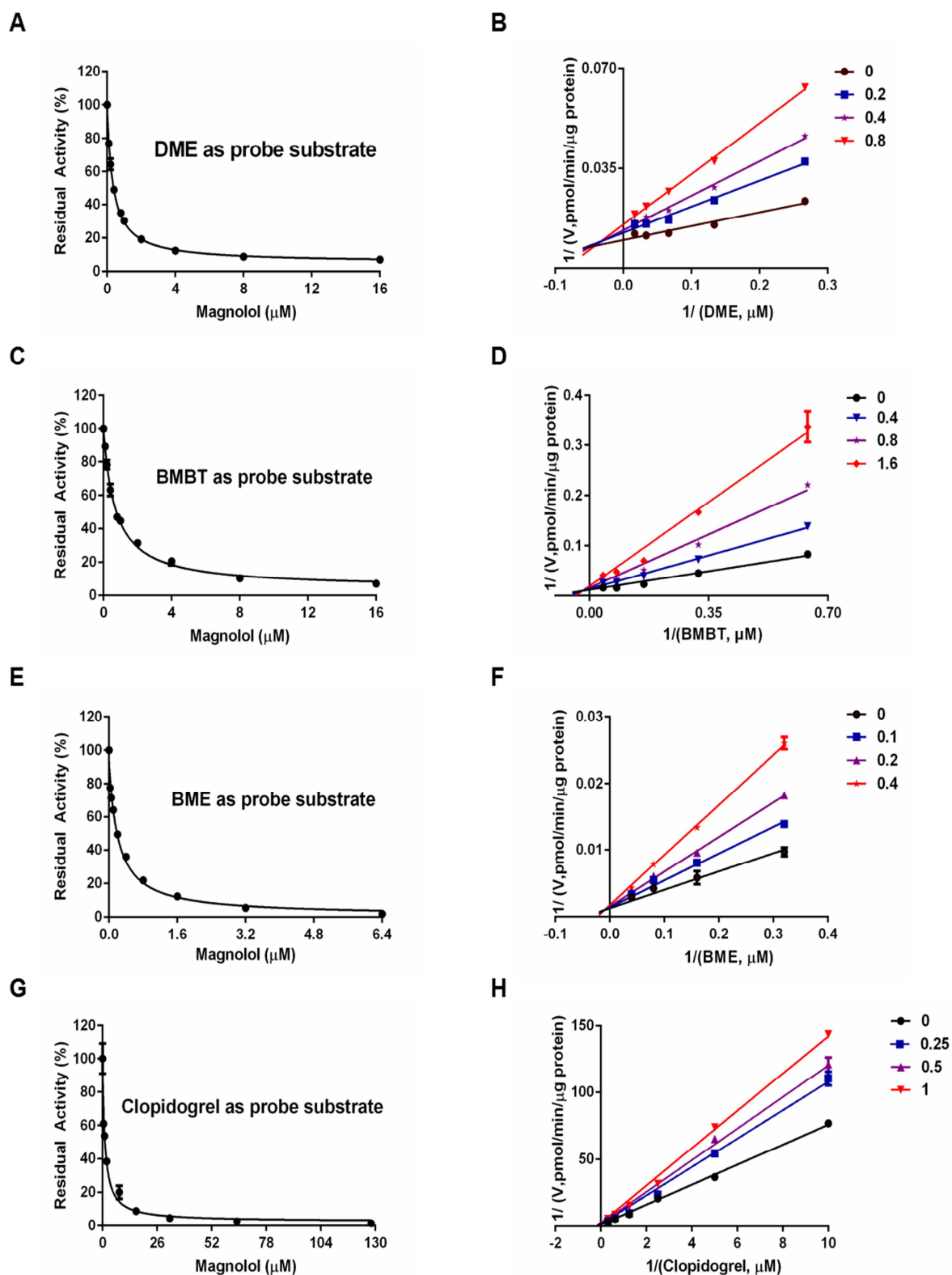


**Fig. 2.** The dose-response inhibition curves of magnolol on hCE1 using DME (A), BMBT (C), BME (E) and clopidogrel (G) as probe substrate, respectively. The Lineweaver-Burk plots for the inhibition of magnolol on hCE1 using DME (B), BMBT (D), BME (F) and clopidogrel (H) as probe substrate, respectively. All data were shown as mean  $\pm$  SD of triplicate determinations.



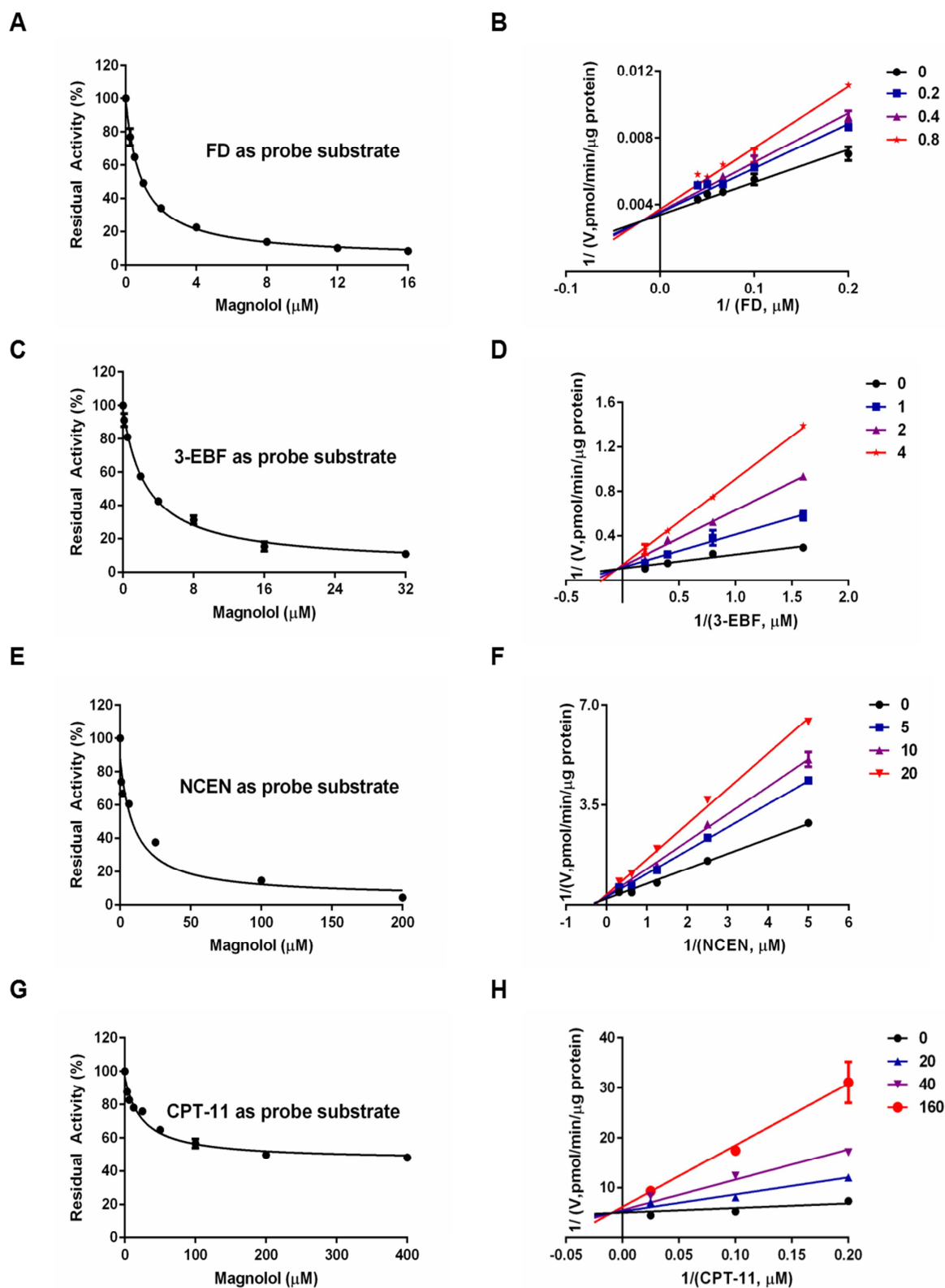


**Fig. 3.** The dose-response inhibition curves of magnolol on hCE2 using FD (A), 3-EBF (C), NCEN (E) and CPT-11 (G) as probe substrate, respectively. The Lineweaver-Burk plots for the inhibition of magnolol on hCE2 using FD (B), 3-EBF (D), NCEN (F) and CPT-11 (H) as probe substrate, respectively. All data were shown as mean  $\pm$  SD of triplicate determinations.

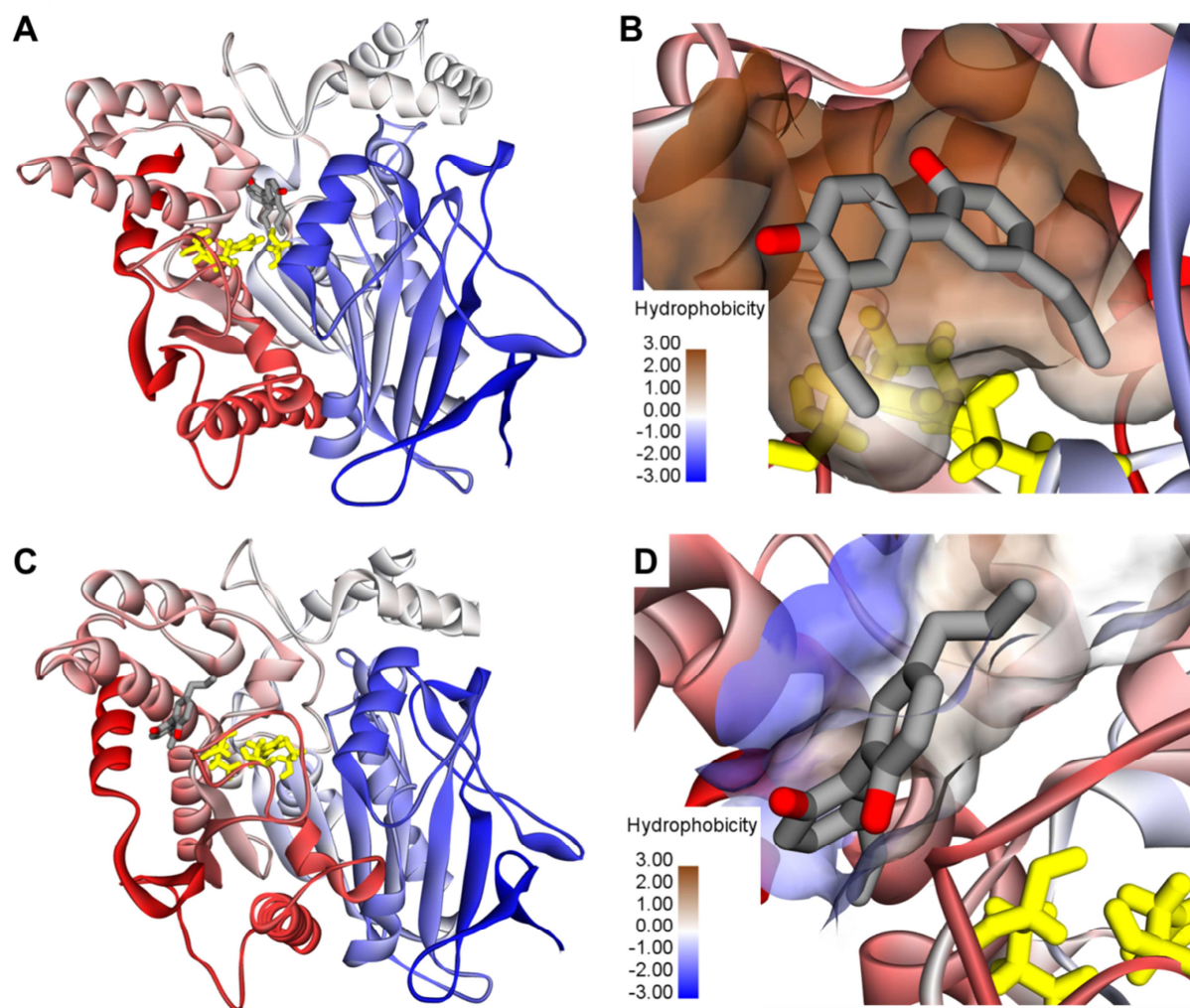


**Fig. 4.** The docking simulations of magnolol into hCE1 (PDB ID: 1MX5). The stereodiagram of magnolol aligned in the active site (A) or the Z-site (C) of hCE1. A detailed view of the binding area of magnolol on the active site (B) or the Z-site (D) of hCE1 with surrounding residues. Note that the catalytic triad of hCE1 (Ser<sup>221</sup>, Glu<sup>354</sup> and His<sup>468</sup>) are colored in yellow, while the surface hydrophobicity scale in right panel is given from brown (3.0) to blue (-3.0).

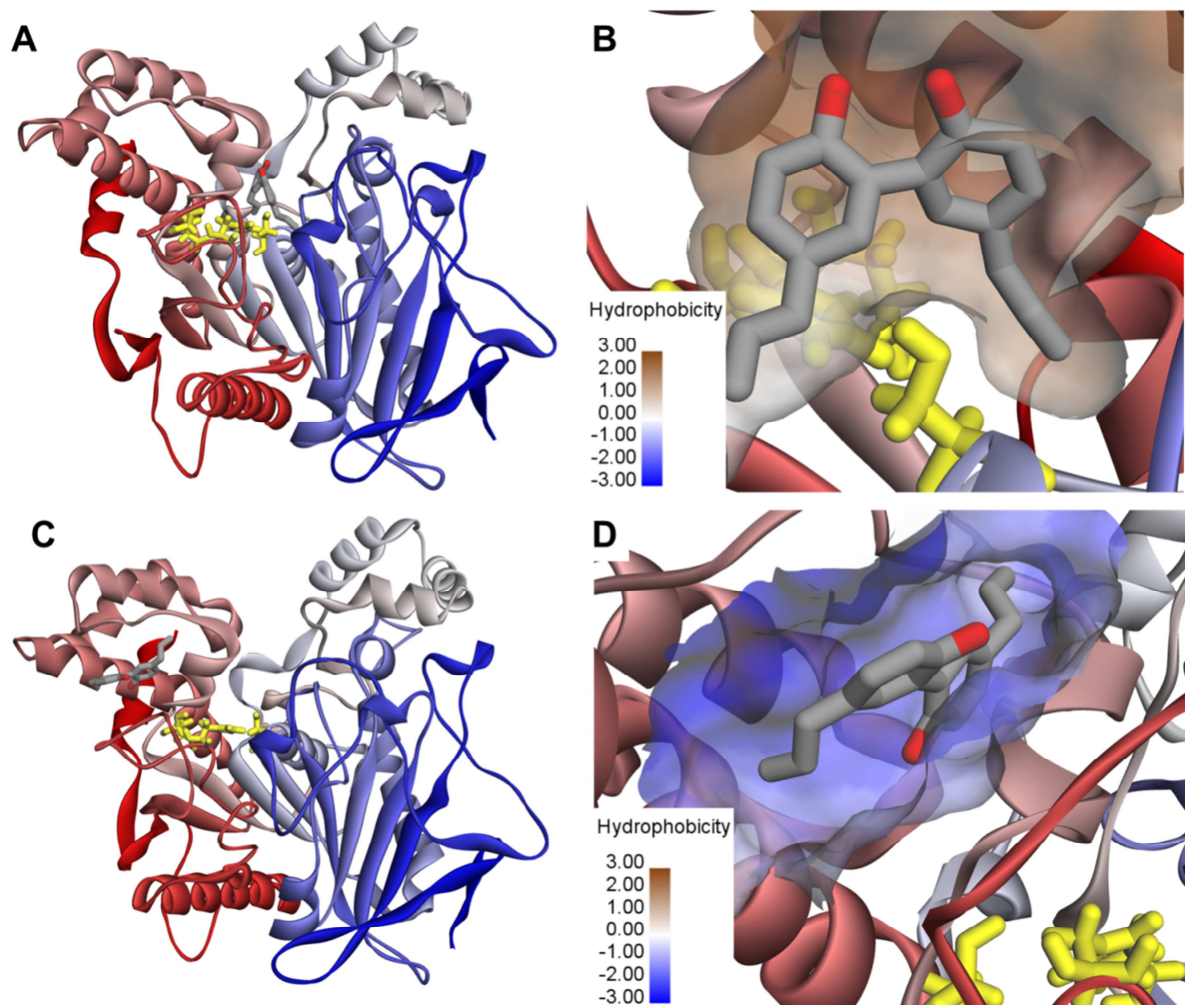


**Fig. 5.** The docking simulations of magnolol into hCE2 (UniProt O00748, build by Swiss-model homology model). The stereodiagram of magnolol aligned in the active site (A) or the Z-site (C) of hCE2. A detailed view of the binding area of magnolol on the active site (B) or the Z-site (D) of hCE2 with surrounding residues. Note that the catalytic triad of hCE2 (Ser<sup>228</sup>, Glu<sup>345</sup> and His<sup>457</sup>) are colored in yellow, while the surface hydrophobicity scale in right panel is given from brown (3.0) to blue (-3.0).

**Highlights**

1. Magnolol strongly inhibits hCE1-mediated hydrolysis of various substrates but inhibits hCE2 in a substrate-dependent manner.
2. Magnolol is cell membrane permeable and capable of inhibiting the intracellular hCE1 in living cells.
3. Magnolol inhibits both hCE1 and hCE2 in a mixed manner.
4. Magnolol could bind on hCE1 at two distinct ligand-binding sites.

**Declaration of interests**

The authors declare that they have no known competing financial interests or personal relationships that could have appeared to influence the work reported in this paper.

The authors declare the following financial interests/personal relationships which may be considered as potential competing interests:

The authors declare no conflict of interest